Available online at www.sciencedirect.com
ScienceDirect
Ceramics International 34 (2008) 1495–1502
CERAMICS INTERNATIONAL
www.elsevier.com/locate/ceramint

Microstructural and compositional aspects of ZnO-based varistor ceramics prepared by direct mixing of the constituent phases and high-energy milling

S. Bernik [a,*], G. Branković [b], S. Rustja [a], M. Žunić [b], M. Podlogar [a], Z. Branković [b]

[a] *Jožef Stefan Institute, Jamova 39, 1000 Ljubljana, Slovenia*
[b] *Center for Multidisciplinary Studies, University of Belgrade, Kneza Višeslava 1a, 11000 Belgrade, Serbia*

Received 11 October 2006; received in revised form 10 March 2007; accepted 6 April 2007
Available online 3 May 2007

Abstract

ZnO-based varistor samples were prepared by the direct mixing of the constituent phases (DMCP) and sintering at 1100 °C for 2 h. The influence of the starting powder mixture's composition – the amounts of the pre-reacted varistor compounds and their composition – and its preparation, either with or without mechano-chemical activation (MCA), on the microstructure, phase composition and electrical characteristics of the varistor samples was studied. It showed that MCA improved the density and microstructural homogeneity of the varistor samples. MCA strongly affected the grain growth: it enhanced the nucleation of inversion boundaries (IBs) in the ZnO grains and the IBs-induced grain-growth mechanism resulted in uniform grain growth and hence a microstructure with smaller ZnO grains and a narrower grain size distribution. The final phase composition of the samples prepared by the DMCP method mainly depended on the presence of varistor dopants that can prevent the formation of the pyrochlore phase, especially Cr_2O_3, while MCA can affect it mostly by providing a homogeneous distribution of those dopants. The DMCP varistor samples prepared with MCA had much better current–voltage characteristics than the samples of the same composition prepared from unactivated powders.

Keywords: B. Microstructure-final; C. Electrical properties; E. Varistors; High-energy milling

1. Introduction

The sintering of ZnO doped with a relatively small amount – a few mol% – of dopants, typically oxides of Bi, Sb, Co, Mn, Ni and Cr, results in ZnO ceramics with an exceptional nonlinearity of the current–voltage characteristics and a high energy-absorption capability. Hence, ZnO-based varistors are extensively used for the over-voltage protection of electrical appliances and electronic equipment, and for the voltage stabilization of electrical power lines. As the current–voltage nonlinearity is a grain boundary phenomenon – the breakdown voltage of a varistor ZnO–ZnO grain boundary is about 3 V – tailoring the microstructure, i.e., the ZnO grain size, of the varistor ceramics is essential for achieving the required breakdown voltage with the right thickness of varistor [1]. Each of the dopants added to the ZnO powder play a distinctive role in providing the varistor characteristics to the sintered ZnO-based ceramic. Bi_2O_3 is essential for inducing the nonlinearity to the ZnO ceramics [2–4]. Sb_2O_3 is a standard additive for controlling the grain growth. The addition of Sb_2O_3 results in the formation of the $Zn_7Sb_2O_{12}$ spinel-type phase, to which the inhibition of the grain growth is generally assigned [5–7]. Doping of the ZnO with Sb_2O_3 also results in the formation of inversion boundaries (IBs) [8]. Recent findings revealed that IBs play a crucial role via the so-called IBs-induced grain-growth mechanism in the grain growth and microstructure development of varistor ceramics [9–11]. Oxides of Co, Mn and Ni incorporate into the grains of ZnO and increase their conductivity. Hence, an optimum distribution of the dopants has to be achieved in the ZnO matrix, both along the grain boundaries and in the grains in order to obtain the best functional characteristics of the varistor ceramics. The homogeneity of the starting oxide mixture is therefore of key importance for the preparation of high-quality varistor ceramics.

* Corresponding author. Tel.: +386 1 4773 682; fax: +386 1 4773 221.
E-mail address: slavko.bernik@ijs.si (S. Bernik).

0272-8842/$34.00
doi:10.1016/j.ceramint.2007.04.003

Typically, the standard ceramic procedure of mixing ZnO with varistor dopants is used for the processing of varistor ceramics. In previous years several alternatives to this procedure were reported, mostly based on the wet-chemical approach (sol–gel method, precipitation from colloidal suspension, etc.) [12–16] and also combustion synthesis [17] which are supposed to provide a highly reactive and fine starting powder mixture with a homogeneous distribution of relatively small amounts of dopants in the matrix of the ZnO. However, in such a complex system, with at least six or more dopants added to the ZnO, a separate precipitation and segregation of dopants can easily occur even when stable solutions are mixed together, causing a poor homogeneity of the powder mixture. Also, they are too costly and demanding for commercial production.

High-energy milling of the starting powder mixture was also reported in previous years as a promising method for the preparation of varistor ceramics [18–20]. The advantage of this approach is that the processing of varistor ceramics is more or less the same as in the case of the standard ceramic procedure except that homogenization with low-energy milling is replaced or proceeded by high-energy dry milling. It was also reported that mechanical activation reduces the weight loss due to the volatilization of Bi_2O_3 and Sb_2O_3 [21].

In all these procedures discussed above pellets that enter into the final stage of sintering to produce varistor ceramics are made from an oxide mixture of ZnO and varistor dopants. In the process of sintering the typical microstructure of a varistor ceramic, composed of ZnO phase, Bi_2O_3-rich liquid phase and $Zn_7Sb_2O_{12}$-type spinel phase, is formed [22]. Branković et al.[23] reported a novel approach to preparing varistor ceramics by sintering a mixture of constituent phases—pre-reacted ZnO doped with oxides of Co and Mn, pre-reacted γ-Bi_2O_3 stabilized with Mn^{2+} or Zn^{2+} and a pre-reacted spinel phase of the $Zn_7Sb_2O_{12}$ type containing other varistor dopants. They referred to the method as a ‘‘direct mixing of constituent phases’’ or shortly DMCP. A varistor prepared by the DMCP method has good nonlinear characteristics; however, intensive milling of the starting mixture results in improved microstructural homogeneity and a higher density of varistor ceramics in comparison to samples prepared using a standard homogenization. The electrical properties of the varistors prepared by the DMCP method are also strongly influenced by the composition of the pre-reacted spinel phase that enters into the starting mixture. While the phase composition remains the same, the varistor dopants that are initially present in the spinel phase redistribute in the microstructure during sintering, which affects the final properties of the varistor ceramics [24].

In this work the compositional and microstructural aspects of the processing of varistor ceramics by combining the DMCP method with a mechanical activation of the starting mixture were studied; the influence of the starting mixture’s composition and the composition of the phases entering the starting mixture on the microstructure development, the grain growth, the phase composition, the distribution of varistor dopants and the current–voltage characteristics of varistor ceramics prepared by the DMCP method was thoroughly analysed and compared for samples prepared using standard milling or mechanically activated by high-energy ball milling.

Table 1
Starting compositions of the samples (wt.% of pre-reacted phases)

Sample label	ZnO (wt.%)	Spinel phase (wt.%)		γ-Bi_2O_3 (wt.%)
		SSP	CSP	
ZC	85	10		5
Z12	85		10	5
Z13	92.5		5	2.5
Z14	95		2.5	2.5
Z15	92.5		2.5	5

2. Experimental procedures

Samples were prepared by mixing powders of phases that are commonly present in varistor ceramics, the ZnO phase, the γ-Bi_2O_3 phase and the $Zn_7Sb_2O_{12}$-type spinel phase, in different amounts appropriate for a certain starting composition. The starting compositions of the samples are given in Table 1 (amounts of the pre-reacted phases in wt.%) and Table 2 (recalculated in equivalent amounts of oxides). It should be pointed out that in all samples the ZnO represents more than 97 mol%; however, there are significant differences among the samples in terms of the amount of Bi_2O_3 and Sb_2O_3; depending on the samples’ composition the Bi_2O_3 can be either at 0.45 or 0.90 mol%, while the Sb_2O_3 can be at about 0.21, 0.42, 0.64 or 0.86 mol%, so that the Sb_2O_3-to-Bi_2O_3 ratio in all the samples is below 1 at 0.95, 0.7, 0.48 or 0.24. While the ZnO phase was prepared using the wet-chemical method, the other two constituent phases were prepared with a classical ceramic procedure from analytical grade oxides mixed in an appropriate ratio for the composition [23,24]. The ZnO powder was added to a solution of Co(II)-nitrate and Mn(II)-acetate with

Table 2
Compositions of starting mixtures from pre-reacted varistor phases recalculated in equivalent amounts of mol% or wt.% of oxides

Sample	ZnO		Bi_2O_3		Sb_2O_3		Co_3O_4		MnO_2		NiO		Cr_2O_3	
	mol%	wt.%	mol%	wt.%	mol%	wt.%	mol%	wt.%	mol%	wt.%	mol%	wt.%	mol%	wt.%
ZC	97.31	90.12	0.91	4.85	0.64	3.42	0.26	1.38	0.05	0.24	0	0	0	0
Z12	96.97	90.65	0.91	4.85	0.86	2.88	0.06	0.17	0.53	0.53	0.28	0.24	0.39	0.68
Z13	98.47	95.22	0.44	2.42	0.42	1.44	0.05	0.13	0.31	0.32	0.14	0.12	0.19	0.34
Z14	98.92	96.26	0.44	2.42	0.21	0.72	0.04	0.12	0.24	0.25	0.07	0.06	0.09	0.17
Z15	98.38	93.77	0.89	4.85	0.21	0.72	0.04	0.11	0.31	0.32	0.07	0.06	0.10	0.17

concentrations of Mn^{2+} and Co^{2+} appropriate for doping the ZnO with 0.1 mol% of each cation. After drying of the suspension, the powder mixture for the ZnO(Co,Mn) phase was pre-reacted at 800 °C for 4 h. The γ-Bi_2O_3 phase with a Bi_2O_3:MnO_2 ratio of 6:1 (labeled as GBO) was prepared by sintering at 800 °C for 6 h. Two different compositions of the $Zn_7Sb_2O_{12}$-type spinel phase were prepared: one doped only with Co_3O_4, having the composition $Zn_{1.46}Co_{0.46}Sb_{0.67}O_{4-\delta}$ (labeled SSP), and a more complex one, doped with oxides of Co, Mn, Ni and Cr, having the composition $Zn_{1.971}Ni_{0.090}Cr_{0.247}Mn_{0.090}Co_{0.030}Sb_{0.545}O_{4-\delta}$ (labeled CSP). The spinel phase was obtained by sintering the samples with an appropriate composition at 1100 °C. Successful preparation of the precursor phases was confirmed by X-ray diffraction (XRD) analysis. The pre-reacted phases were ground in an agate mortar into a fine powder. The starting powder mixtures from the pre-reacted phases in proper ratios for a given composition were initially homogenized in an agate planetary ball mill in absolute ethanol for 2 h and dried. A share of each starting mixture was subsequently also mechanically activated by intensive dry milling in an agate planetary ball mill under the following conditions: milling intensity = 340 rotations/min; time = 2 h; balls-to-powder weight ratio = 20:1. In order to distinguish between the samples of the same composition that were differently treated, the labels of the mechanically activated samples contain an additional ''m'' at the end, which is missing from the labels of the unactivated samples (i.e., Z12m versus Z12).

The powders were uni-axially pressed with a pressure of 200 MPa into pellets with a diameter of 10 mm and a thickness of 1.5 mm. They were air sintered at 1100 °C for 2 h. Microstructures of the samples were analyzed and their current–voltage characteristics were measured. For the microstructural analysis cross-sections of the samples (pellets) were ground and polished. Part of the microstructure of each sample was etched in dilute hydrochloric acid (solution HCl (conc.):H_2O = 1:40; etching time = about 5 s) to expose the grain boundaries and hence the ZnO grains for the stereological analysis. The other polished (un-etched) part of the microstructure was used to analyze the phase composition of the sample. The microstructures were examined using a scanning electron microscope, (SEM) JEOL JSM-5800, equipped with an EDXS detector and the Oxford Instruments Link Isis 300 analytical system, in back-scattered electron (BE) mode. The phase compositions of the samples and the compositions of the individual phases were determined in the SEM by energy-dispersive X-ray spectroscopy (EDXS) analysis. Several EDXS measurements of each phase were made per sample in the un-etched area of the microstructure to obtain an average composition of the phase and to assess the distribution of the dopant in the sample. It has to be considered, however, that the detection limit of the EDXS analysis is generally about 0.1 wt.%. Also, secondary phases in the varistor ceramics are micrometer and sub-micrometer in size, and it is very likely that the signal is not taken only from the analyzed phase, but also from the neighboring phases, mostly from the ZnO phase. BE images taken from the etched area of the samples' microstructure, where grain boundaries and hence grains are clearly evident, were used for the stereological analysis. The average ZnO grain size (D) and the grain size distribution were determined for each sample from measurements of 500–1000 grains per sample. The surface of each grain was measured and its size was calculated in terms of a diameter for a circular geometry.

For the current–voltage (I–V) characterization of the samples with a direct-current method using Voltcraft MXD-4660A digital multimeter, silver electrodes were deposited on the parallel sides of the pellet and sintered at 600 °C. The breakdown voltage, i.e., the nominal varistor voltage (V_N), of the samples was determined at 1 mA/cm^2, and a leakage current (I_L) at a voltage of 0.8 V_N. The nonlinear coefficient (α) was determined for the current range 1.0–10 mA/cm^2.

3. Results and discussion

Mechano-chemical activation (MCA) influences the morphology of the starting powder, and significantly reduces the particles' sizes and also their compactness in comparison to the untreated powder. Additionally, MCA used in a ''direct mixing of constituent phases'' (DMCP) preparation method improves the uniformity of distribution of the phases in the starting mixture, and results in a better compositional homogeneity of the starting powder mixture. SEM images of the powders with the composition Z12, untreated or mechanically activated, are shown in Fig. 1; while from the SE images Fig. 1a and c the differences in the morphology are clearly evident, the BE images Fig. 1b and d indicate the differences in compositional homogeneity between the untreated and mechanically activated powders.

Microstructures of the varistor samples sintered at 1100 °C for 1 h are presented in Fig. 2. The microstructures of the varistor samples prepared from the MCA powders appear more homogeneous, with a finer distribution of the secondary phases, lower porosity and mostly a smaller or the same ZnO grain size with a more uniform size distribution, in comparison to the sample prepared from the unactivated powders. The results of the stereological analysis of the ZnO grain size and the grain size distribution confirmed these general microstructural observations. The average ZnO grain sizes of the samples from the MCA powders are about 10–40% smaller in comparison to the samples with the same composition from unactivated powders, except for the samples Z14 and Z14m. The results of the ZnO grain size and the size distribution analysis are presented in Table 3.

Microstructural examinations also showed the obvious presence of inversion boundaries (IBs) in most of the ZnO grains of the samples from MCA powders, regardless of the amount of Sb_2O_3 in the sample, while in the samples from unactivated powders the IBs are very difficult to see, especially in the samples with the lowest content of Sb_2O_3. Sb_2O_3 is the dopant that triggers the formation of IBs in the ZnO grains, and we showed that IBs strongly influence the grain growth process and microstructure development via the so-called IBs-induced grain-growth mechanism [9–11]. In the early stage of sintering the Sb_2O_3 triggers the nucleation of IBs in some ZnO grains (nuclei), which exhibit a preferential growth and grow at the expense of the normal ZnO grains until they impinge on each

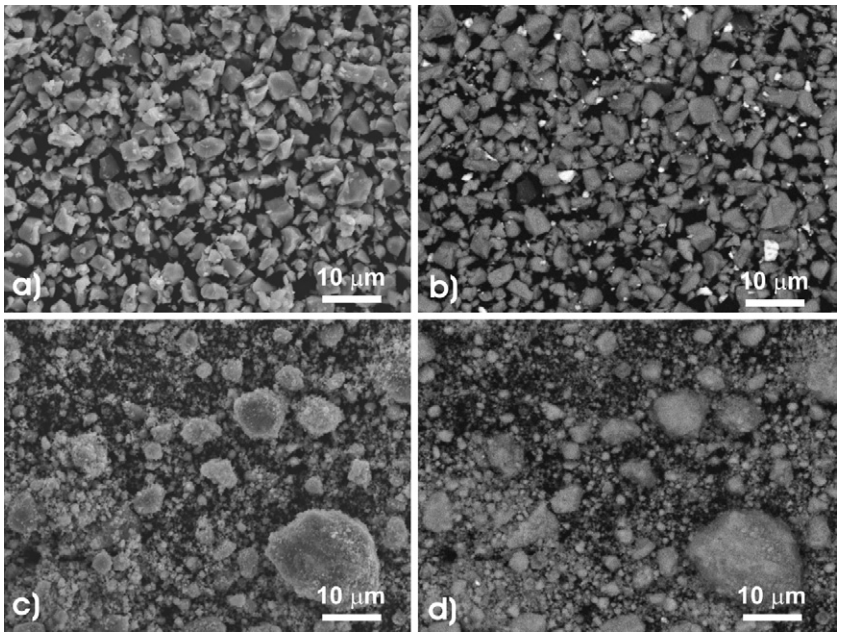

Fig. 1. Microstructures of untreated powder Z12 in (a) SE mode and (b) BE mode, and mechanically treated powder Z12m in (c) SE mode and (d) BE mode, respectively.

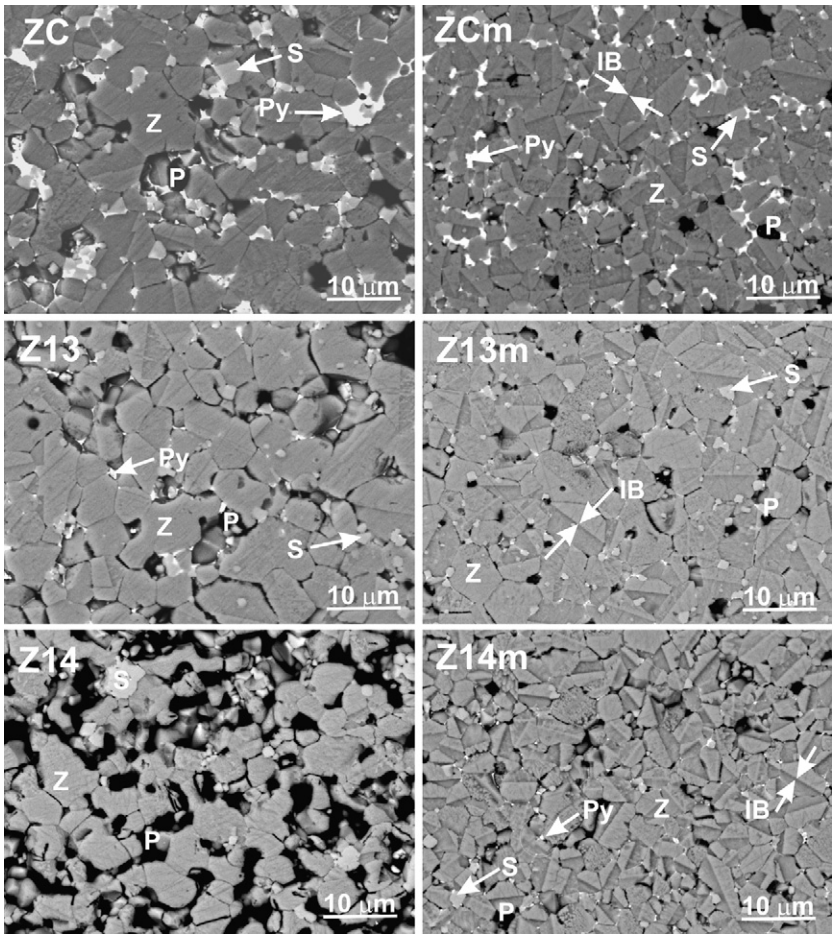

Fig. 2. Backscattered electron (BE) images from scanning electron microscope (SEM) of etched microstructures of untreated and mechanically treated varistor samples sintered at 1100 °C for 1 h. Z: ZnO phase; S: $Zn_7Sb_2O_{12}$ spinel-type phase; Py: pyrochlore phase; P: pore; IB: inversion boundary.

Table 3
Relative density (ρ/ρ_T), average ZnO grain size (D), its standard deviation and basic current–voltage (I–V) characteristics of the varistor samples prepared by the DMCP method and without or with mechano-chemical activation of starting powder mixture, sintered at 1100 °C for 1 h

Sample	ρ/ρ_T (%)	D (μm)	σ_D (μm/%)	V_T (V/mm)	V_{GB} (V)	α	I_L (μA)
ZC	88	3.6	1.8/50	357	1.3	46	10
ZCm	93	3.1	1.4/45	668	2.1	60	5
Z12	90	4.2	1.8/43	484	2.0	46	4
Z12m	91	2.4	1.1/45	824	2.0	53	2
Z13	89	4.4	2.3/52	443	2.0	38	10
Z13m	98	4.0	1.8/45	527	2.1	50	6
Z14	89	2.8	1.8/64	437	1.2	32	79
Z14m	95	2.9	1.3/45	507	1.5	44	8
Z15	89	3.1	2.0/64	416	1.3	29	120
Z15m	97	2.7	1.2/44	426	1.2	35	20

other and completely prevail in the microstructure when the growth is slowed. The nucleation of IBs and hence their number in the early stage of sintering depends on the amount of Sb_2O_3. For a small number of ZnO grains infected by IBs, these nuclei can grow to large sizes before they prevail in the microstructure, which is consequently coarse grained, while in the case of a large number of nuclei they cannot grow much before they impinge on each other and the microstructure is fine grained. The results indicate that MCA influences the nucleation of IBs in the ZnO grains, which can only explain the difference in the occurrence of IBs in samples with otherwise the same composition and hence also the amount of Sb_2O_3 added with the pre-reacted $Zn_7Sb_2O_{12}$ spinel phase. The finer grain size of the MCA powders and the homogeneous distribution of the phases also ensure the uniform presence of the fine $Zn_7Sb_2O_{12}$ phase as a source of Sb_2O_3 everywhere in the starting mixture, which all contributes to its enhanced dissolution in the Bi_2O_3-rich phase. Consequently, at the same starting composition the availability of the Sb_2O_3 for the nucleation of IBs in the ZnO grains of MCA powders is increased in comparison to the unactivated powders. In addition, it is reasonable to expect that MCA increases the number of defects in the ZnO grains, which can also contribute to the enhanced nucleation of IBs in the ZnO grains [25]. The differences in the microstructures between the samples from MCA powders and the unactivated powders of the same starting composition can to some extent result from the different morphology, particle size and compactness, as well as the homogeneity of the powders, which definitely influenced their sinterability and hence their density, phase distribution and also the phase composition. However, in the samples prepared from MCA powders the grain growth was evidently strongly influenced by the IBs, which are present in all ZnO grains; the enhanced nucleation of IBs in more ZnO grains at the early stage of sintering resulted, in accordance with the IBs-induced grain-growth mechanism [9–11,25], in a microstructure with a smaller average ZnO grain size and a narrower grain size distribution than in the samples with the same composition from unactivated powders where the IBs in the ZnO grains are hardly present.

The starting powders of the samples were made by mixing together in different proportions the pre-reacted ZnO phase, the $Zn_7Sb_2O_{12}$ spinel-type phase, and the γ-Bi_2O_3 phase mixed (Table 1). The microstructural analysis showed, as was to be expected, the presence of these phases also in the samples after sintering at 1100 °C. Identity of the phases was confirmed by EDXS analysis. In addition, a $Bi_3Zn_2Sb_3O_{14}$ pyrochlore-type phase was also observed in the samples. The chemistry of the pyrochlore phase in the ZnO-based varistor ceramics doped with Bi_2O_3, Sb_2O_3 and other varistor dopants is well known [26,27]. The appearance of the pyrochlore phase can be explained by the dissolving of the $Zn_7Sb_2O_{12}$ spinel phase in the Bi_2O_3-rich phase at the sintering temperature, which can subsequently result in the formation of the pyrochlore phase during cooling. While in samples ZC and ZCm the pyrochlore phase is the major Bi_2O_3-containing phase, and only traces of Bi_2O_3-rich phase could be observed, no pyrochlore phase was detected in the samples Z12 and Z12m. The compositions of the samples in mol% of oxides are given in Table 2. The composition Z12 contains a relatively large amount of Cr_2O_3, which can explain the absence of the pyrochlore phase in the varistor samples with this composition. In contrast, the ZC compositions are without Cr_2O_3, hence most of the Bi_2O_3 is bounded in the pyrochlore phase. The compositions Z14 and Z15 contain relatively small amounts of Cr_2O_3. Consequently, in the samples with these two compositions the pyrochlore phase and the Bi_2O_3-rich phase are present in relatively equal amounts. The composition Z13 contains a medium amount of Cr_2O_3 in comparison to the other Cr_2O_3-containing compositions. While in sample Z13, made from unactivated powder, the Bi_2O_3 phase and the pyrochlore phase seem to be present in similar amounts, only traces of the pyrochlore phase can be observed in the Z13m sample prepared from MCA powder. The results indicate that the amount of Cr_2O_3 in the Z13 composition is somehow just on the edge of the amount needed to effectively prevent the formation of the pyrochlore phase; a more uniform distribution of the Cr_2O_3 in sample Z13m prepared from MCA powder can result in less pyrochlore phase in comparison to the Z13 sample prepared from unactivated powder where the same amount of Cr_2O_3 is not distributed evenly. Microstructures of the ZC samples, with the pyrochlore phase, and Z15m, with the Bi_2O_3 phase and traces of the pyrochlore phase, are presented in Fig. 3.

The results indicated that MCA has a limited influence on the phase composition of the samples prepared by the DMCP method. The phase composition of the varistor samples prepared by the DMCP method is largely pre-determined by

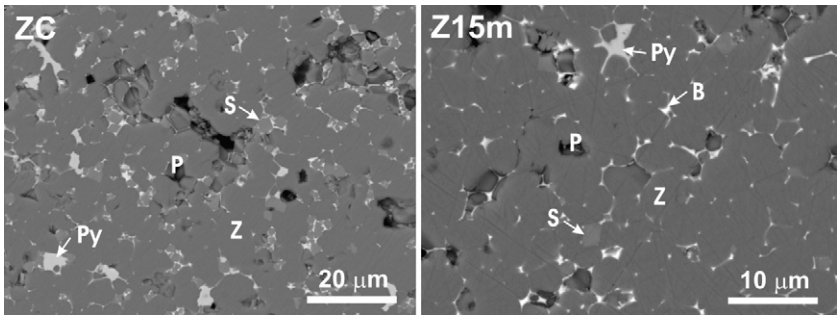

Fig. 3. Backscattered electron (BE) images from SEM of microstrucrures of varistor samples ZC and Z15m sintered at 1100 °C. Z: ZnO; B: Bi_2O_3-rich phase; Py: pyrochlore phase; S: spinel phase; P: pore.

the phases present in the starting powder mixture. However, the final phase composition obtained in the samples after sintering actually depends on the presence and the amount of those dopants that influence the formation of the pyrochlore phase on cooling from the sintering temperature. In this regard the role of Cr_2O_3, which stabilizes the spinel phase and prevents formation of the pyrochlore phase, is particularly crucial [27]. MCA can effect the final phase composition of the samples mainly by providing a uniform distribution of the dopants, which helps in preventing the formation of the pyrochlore phase, especially for low amounts of Cr_2O_3 in the samples, when its distribution is even more critical. When the formation of the pyrochlore phase is completely prevented, the ratios of the constituent phases from the starting powder mixture remain in the samples also after sintering. However, the occurrence of the pyrochlore phase means that the amounts of the $Zn_7Sb_2O_{12}$ spinel phase and the Bi_2O_3-rich phase in the sintered samples were reduced in comparison to the starting composition. The presence of the Bi_2O_3 phase at the grain boundaries is essential for the nonlinearity of the ZnO-based varistor ceramics; hence, a decrease in the amount of the Bi_2O_3-rich phase and its partial or full replacement by the varistor-non-active pyrochlore phase can influence the electrical characteristics of the samples.

Another important aspect is the distribution of varistor dopants in the sample. Oxides of Bi_2O_3 and Sb_2O_3 (ZnO as a component in excess is not considered) are mostly influenced by the equilibria among the Bi_2O_3-rich phase, the $Zn_7Sb_2O_{12}$ spinel phase and the $Bi_3Zn_2Sb_3O_{14}$ pyrochlore phase, which is discussed above. Redistribution of the other varistor dopants – cations of Co, Mn, Ni and Cr – among the phases present in the sample also takes place during the sintering process. Evidently, this could be expected when the pyrochlore phase occurs after sintering in addition to the initially present phases in the samples prepared by the DMCP method. However, the redistribution of the dopants also probably appears in the case that the phase composition and the ratios of these phases from the starting mixture prepared by the DMCP method is prevented in samples after sintering. Results of the EDS analysis of the spinel phase confirmed these assumptions. For the starting mixture of the samples ZC and ZCm the pre-reacted spinel phase SSP was used, containing only Co as a dopant. However, after sintering the spinel phase in these samples contains significantly less Co and also Mn, which can originate either from the ZnO phase or from the Bi_2O_3-rich phase, most likely from the Bi_2O_3-rich phase. Similarly in the other samples for which the pre-reacted CSP spinel phase, containing Co, Mn, Ni and Cr as dopants, was used, the spinel phase after sintering contains less Co, Ni and Cr than the initial CSP composition, but clearly more Mn. The Co and Mn were also detected in the $Bi_3Zn_2Sb_3O_{14}$ pyrochlore-type phase, while Cr was detected in the Bi_2O_3-rich phase. It is important to consider the redistribution of the dopants among the phases, especially with regard to the final level of doping of the ZnO phase after sintering to ensure its high conductivity. A comparison of the compositions of the pre-reacting spinel phase, which enters into the starting powder mixture of the samples prepared by the DMCP method, and the average composition of the spinel phase in the sintered samples determined by EDXS analysis is given in Table 4. Results of the EDXS analysis presented in Table 4 do not want to imply that these are exact compositions of the spinel phase in the samples after sintering; they are presented in this way only to indicate the changes in the composition and the redistribution of dopants among the phases during sintering.

The current–voltage (*I–V*) characteristics of the samples are presented in Table 3, while their current density–electric field

Table 4
Compositions of pre-reacted spinel phase used for the preparation of samples by DMCP method and compositions of the spinel phase in samples after sintering obtained by the EDS analysis, normalised on a nine cations per formula unit

Sample	Spinel	Zn	Sb	Co	Mn	Ni	Cr
ZC, ZCm	SSP	5.60	2.02	1.38	0.00	0.00	0.00
	by EDS	6.74 ± 0.11	1.81 ± 0.06	0.36 ± 0.01	0.04 ± 0.02	0.00	0.00
Z12–15	CSP	5.97	1.65	0.09	0.27	0.27	0.75
Z12m–15 m	by EDS	6.50 ± 0.17	1.39 ± 0.14	0.02 ± 0.02	0.34 ± 0.14	0.16 ± 0.03	0.59 ± 0.06

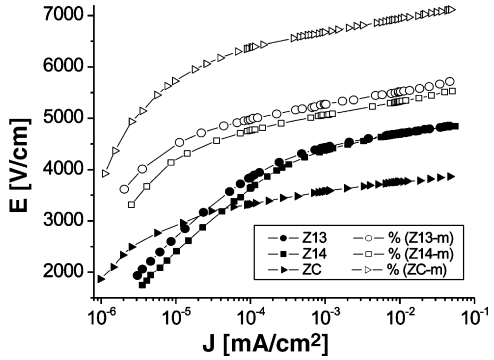

Fig. 4. The current density/electric field (*J–E*) curves of the varistor samples sintered at 1100 °C.

(*J–E*) curves are given in Fig. 4. These results show that the mechano-chemical treatment significantly improved the electrical characteristics of the samples in comparison to the samples of the same composition prepared from the unactivated mixture; it resulted in an increase of the threshold voltage V_T (V/mm) and the nonlinear coefficient α of the samples, and a decrease of the leakage current I_L. In general, the improved electrical characteristics could be attributed to a better microstructural homogeneity – uniform phase distribution, narrower ZnO grain size – and density of the samples prepared from the activated powder mixtures. The increase of V_T can be mainly attributed to the decrease in the average ZnO grain size in the samples prepared from the MCA powder. The importance of the uniform phase distribution in the starting mixture prepared by the DMCP method was particularly clear in the case of the samples Z14 and Z15, with the small amount of pre-reacted $Zn_7Sb_2O_{12}$ and γ-Bi_2O_3 phases mixed with the ZnO phase and the lowest amount of varistor dopants (oxides of Sb, Co, Mn, Ni and Cr) present in the samples (see Tables 1 and 2). While the samples Z14 and Z15 prepared from the unactivated powder mixture have an extremely high leakage current I_L, samples with the same starting composition prepared from the MCA powders, Z14m and Z15m, have a significantly lower I_L, which can be explained by the homogeneous distribution of the limited amount of available varistor dopants in these samples.

4. Conclusions

ZnO-based varistor samples were prepared by a direct mixing of constituent phases (DMCP) and sintering at 1100 °C for 2 h. The influence of the starting composition – amounts of pre-reacted γ-Bi_2O_3 and $Zn_7Sb_2O_{12}$ spinel-type phase added to the pre-reacted ZnO phase, and the composition of these phases with regard to the amount of oxides of Co, Mn, Ni and Cr – and the preparation of the starting powder mixture either with or without mechano-chemical activation (MCA) on the microstructure, phase composition and current–voltage characteristics of the varistor samples was studied.

Mechano-chemical activation (MCA) influences the morphology of the starting powder, and significantly reduces the particles' sizes and also their compactness in comparison to the untreated powder. Consequently, the microstructures of the varistor samples prepared from the MCA powders appear more homogeneous, with a higher density and a finer distribution of the secondary phases. Grain growth in the samples prepared from MCA powders was strongly influenced by IBs, which are present in all the ZnO grains regardless of the amount of Sb_2O_3 in the sample. The results indicate that MCA enhances the nucleation of IBs in more ZnO grains at the early stage of sintering, which in accordance with the IBs-induced grain-growth mechanism [9–11,25] results in a microstructure with a smaller average ZnO grain size and a narrower grain size distribution than the samples with the same composition prepared from unactivated powders, where the IBs in the ZnO grains are hardly present, especially for the lowest contents of Sb_2O_3.

The phase composition of the varistor samples prepared by the DMCP method is largely pre-determined by the phases present in the starting powder mixture. In addition, the $Bi_3Zn_2Sb_3O_{14}$-type pyrochlore phase can be formed. Consequently, it showed that the final phase composition obtained in the samples after sintering actually depends on the presence and the amount of Cr2O3, which influences the formation of the pyrochlore phase on cooling from the sintering temperature. MCA can effect the final phase composition of the samples, mainly by providing a uniform distribution of Cr_2O_3 (or any other key dopants), which is essential in preventing the formation of the pyrochlore phase, especially for small amounts. The results of the EDS analysis confirmed that during sintering a significant redistribution of the varistor dopants, i.e., the oxides of Co, Mn, Ni and Cr, takes place among the phases in the samples, even in the case that the phase composition from the starting powder mixture is preserved and no pyrochlore phase is formed. This can influence the final level of doping of the ZnO phase and hence its conductivity.

The samples prepared from MCA powders had much better current–voltage characteristics than the samples of the same composition prepared from unactivated powders: a higher threshold voltage, V_T, and nonlinear coefficient, α, and also a much lower leakage current, I_L.

Acknowledgements

The authors acknowledge the financial support by the Slovenian Research Agency (Program Contract no. P2-0084-0106/05 and Grant BI-SCG/05-06/009) and the Serbia and Montenegro Ministry of Science within the bilateral project ''Synthesis of varistor ceramics with significantly reduced amount of dopants and improved microstructural and current–voltage characteristics''.

References

[1] D.R. Clarke, Varistor ceramics, J. Am. Ceram. Soc. 82 (1999) 485–502.
[2] J. Wong, Sintering and varistor characteristics of ZnO–Bi_2O_3, J. Appl. Phys. 51 (1980) 4453–4459.
[3] T. Senda, R.C. Bradt, Grain growth in sintered ZnO and ZnO–Bi_2O_3 ceramics, J. Am. Ceram. Soc. 73 (1990) 106–114.
[4] D. Dey, R.C. Bradt, Grain growth of ZnO during Bi_2O_3 liquid-phase sintering, J. Am. Ceram. Soc. 75 (1992) 2529–2534.

[5] J. Kim, T. Kimura, T. Yamaguchi, Microstructure development in Sb_2O_3-doped ZnO, J. Mater. Sci. 24 (1989) 2581–2586.
[6] M. Ito, M. Tanahashi, M. Uehara, A. Iga, The Sb_2O_3 addition effect on sintering ZnO and ZnO + Bi_2O_3, Jpn. J. Appl. Phys. 36 (Part 2 (11A)) (1997) L1460–L1463.
[7] T. Senda, R.C. Bradt, Grain growth of zinc oxide during the sintering of zinc oxide–antimony oxide ceramics, J. Am. Ceram. Soc. 74 (1991) 1296–1302.
[8] T. Senda, R.C. Bradt, Twinning in ZnO with Sb_2O_3 additions, J. Ceram. Soc. Jpn. 99 (1991) 727–731.
[9] N. Daneu, A. Recnik, S. Bernik, D. Kolar, Microstructural development in SnO-doped ZnO–Bi_2O_3 ceramics, J. Am. Ceram. Soc. 83 (2000) 3165–3171.
[10] N. Daneu, A. Rečnik, S. Bernik, Grain growth control in Sb_2O_3-doped zinc oxide, J. Am. Ceram. Soc. 86 (2003) 1379–1384.
[11] S. Bernik, N. Daneu, A. Rečnik, Inversion boundary induced grain growth in TiO_2 and Sb_2O_3 doped ZnO-based varistor ceramics, J. Eur. Ceram. Soc. 24 (2004) 3703–3708.
[12] N.S. Bell, J. Cesarano, J.A. Voigh, S.J. Lockwood, D.B. Dimos, Colloidal processing of chemically prepared zinc oxide varistors. Part I. Milling and dispersion of powder, J. Mater. Res. 19 (5) (2004) 1333–1340.
[13] N.S. Bell, J.A. Voigh, B.A. Tuttle, D.B. Dimos, Colloidal processing of chemically prepared zinc oxide varistors. Part II. Near-net-shape forming and fired electrical properties, J. Mater. Res. 19 (5) (2004) 1341–1347.
[14] X.Y. Kang, M.J. Tu, M. Zhang, T.D. Wang, Microstructure and electrical properties of doped ZnO varistor nanomaterials, functional nanomaterials for optoelectronics and other applications, Solid State Phenom. 99–100 (2004) 127–132.
[15] S.Y. Chu, T.M. Yan, S.L. Chen, Analysis of ZnO varistors prepared by the sol–gel method, Ceram. Int. 26 (2000) 733–737.
[16] X.Y. Kang, H. Yin, T.M. De, T.M. Jing, Analysis of ZnO varistors prepared from nanosize ZnO precursors, Mater. Res. Bull. 33 (11) (1998) 1703–1708.
[17] V.C. de Sousa, M.R. Morelli, R.H.G.A. Kiminami, M.S. Castro, Electrical properties of ZnO-based varistors prepared by combustion synthesis, J. Mater. Sci.: Mater. Electron. 13 (2002) 319–325.
[18] S. Boily, H.D. Alamdari, G. Cross, A. Jolly, A. VanNeste, P. Grutter, R. Schulz, Ball milled ZnO for varistor application, synthesis and properties of mechanically alloyed and nanocrystalline materials, Pts 1 and 2—ISMANAM'96, Mater. Sci. Forum 235 (Part 1 & 2) (1997) 993–998.
[19] H.D. Alamdari, S. Boily, M. Blouin, A. VanNeste, R. Schulz, High energy ball milled nanocrystalline ZnO varistors, metastable, mechanically alloyed and nanocrystalline materials, pts 1 and 2, Mater. Sci. Forum 343–343 (Part 1 & 2) (2000) 909–917.
[20] C.P. Fah, J. Wang, Effect of high-energy mechanical activation on the microstructure and electrical properties of ZnO-based varistors, Solid State Ionics 132 (2000) 107–117.
[21] C. Gomez-Yanez, J. Velazquez-Morales, E.G. Palacios, Mechanical activation of spinel and pyrochlore phases in ZnO based varistors, J. Electroceram. 13 (2004) 745–750.
[22] M. Inada, Effect of heat-treatment on crystal phases, microstructure and electrical properties of nonohmic zinc oxide ceramics, Jpn. J. Appl. Phys. 18 (8) (1979) 1439–1446.
[23] Z. Branković, O. Milošević, D. Poleti, L. Karanović, D. Uskoković, ZnO varistors prepared by direct mixing of constituent phases, Mater. Trans. JIM 41 (9) (2000) 1226–1231.
[24] Z. Branković, G. Branković, D. Poleti, J.A. Varela, Structural and electrical properties of ZnO varistors containing different spinel phases, Ceram. Int. 27 (2001) 115–122.
[25] A. Rečnik, N. Daneu, S. Bernik, Nucleation and growth of basal-plane inversion boundaries in ZnO, J. Eur. Ceram. Soc. 27 (2007) 1999–2008.
[26] M. Inada, Formation mechanism of nonohmic zinc oxide ceramics, Jpn. J. Appl. Phys. 19 (3) (1980) 409–419.
[27] S.G. Cho, H. Lee, H.S. Kim, Effect of chromium on the phase evolution and microstructure of ZnO doped with bismuth and antymony, J. Mater. Sci. 32 (1997) 4283–4287.